Article

Marine Sulfated Glycans Inhibit the Interaction of Glycosaminoglycans with SARS-CoV-2 Omicron XBB Variant S-Protein

Peng He[1,2], Yuefan Song[1,2], Weihua Jin[1,3], Yunran Li[1,2], Ke Xia[1,2], Seon Beom Kim[4,5], Rohini Dwivedi[4], Marwa Farrag[4], John Bates,[4] Vitor H. Pomin[4], Robert J. Linhardt[1,2,6], Jonathan S. Dordick[1,6*], and Fuming Zhang[1,6*]

1 Center for Biotechnology and Interdisciplinary Studies, Rensselaer Polytechnic Institute, Troy, NY, United States
2 Department of Chemistry and Chemical Biology, Rensselaer Polytechnic Institute, Troy, NY 12180, USA
3 College of Biotechnology and Bioengineering, Zhejiang University of Technology, Hangzhou 310014, China
4 Department of BioMolecular Sciences, Research Institute of Pharmaceutical Sciences, The University of Mississippi, Oxford, MS, United States
5 Department of Food Science & Technology, College of Natural Resources and Life Science, Pusan National University, Miryang, Republic of Korea
6 Departments of Chemical and Biological Engineering, Rensselaer Polytechnic Institute, Troy, NY 12180, USA
* Correspondence: dordick@rpi.edu (J.S.D.) and zhangf2@rpi.edu (F.Z.)

Abstract: As many other viruses, SARS-CoV-2 utilizes heparan sulfate (HS) glycosaminoglycan (GAG) on host cell surfaces to facilitate viral attachment and initiate cellular entry through the ACE2 receptor. Therefore, interfering with virion-HS interactions represents a promising target to develop broad-spectrum antiviral therapeutics. Sulfated glycans derived from marine organisms have been proven to be exceptional reservoirs of naturally existing HS mimetics, which exhibit remarkable therapeutic properties encompassing antiviral/microbial, antitumor, anticoagulant, and anti-inflammatory activities. In the current work, interactions between SARS-CoV-2 Spike protein (S-protein) RBD (both WT and XBB.1.5 variants) and heparin were explored to study the inhibitory activity of 10 marine-sourced glycans, three sulfated fucans, three fucosylated chondroitin sulfates and two fucoidans extracted from the sea cucumbers *Isostichopus badionotus*, *Pentacta pygmaea*, and *Holothuria floridana*, the sea urchin *Lytechinus variegatus*, and seaweed *Saccharina japonica*, respectively, as well as two chemically desulfated analogues. Surface plasmon resonance (SPR) was employed to assess the inhibitory activity of these marine sulfated glycans on the interactions between SARS-CoV-2 S-protein and heparin. Wild-type (WT) and Omicron XBB.1.5 S-proteins were found to bind to heparin, a highly sulfated HS. The tested marine-sourced sulfated glycans exhibited strong inhibition of WT and XBB.1.5 S-protein interactions.

Keywords: Marine sulfated glycans; SARS-CoV-2; Omicron XBB.1.5; Spike protein; Heparin

1. Introduction

At the end of 2019, a contagious novel coronavirus emerged and quickly spread across the world resulting in the COVID-19 pandemic. The pandemic is caused by severe acute respiratory syndrome coronavirus 2 (SARS-CoV-2) with more than 762 million confirmed cases and more than 6.8 million deaths as of April 2023, based on the records of World Health Organization [1]. Since 2019, multiple COVID-19 pandemic waves have occurred accompanied by numerous new SARS-CoV-2 variants [2]. According to the US Centers for Disease Control and Prevention (CDC), COVID-19 was the fourth leading cause of death in the United States in 2022 [3]. This virus exhibits a high mutation rate with a positive-sense single-stranded RNA [4]. Mutations on the Spike protein (S-protein) of SARS-CoV-2, which plays critical roles in the binding and entry of SARS-CoV-2 to host cells, have led to five

 doi:10.20944/preprints202305.1749.v1

circulating variants of concern (VOC) - Alpha, Beta, Gamma, Delta and multiple Omicron variants [5].

Among the Omicron variants, XBB.1.5 has been spreading rapidly worldwide during the last several months. As of April 2023, the highly transmissible XBB.1.5 variant was projected to represent at approximately 78% of US infections according to the CDC [6]. The Omicron XBB. 1.5 is a descendent lineage of the XBB (a recombinant of BA.2.10.1 and BA.2.75) family with two mutations (G252V and F486P) in the S-protein [7]. The rare F486P mutation in XBB.1.5 appears to correlate with binding affinity of the S-protein receptor-binding domain to human angiotensin-converting enzyme-2 (RBD/hACE2) complexes, thereby enhancing transmissibility [8]. The higher ACE2 binding affinity and the ability to escape from current monoclonal antibodies accelerated the dominance of XBB.1.5 in many countries.

Anionic glycans such as heparan sulfate (HS), chondroitin sulfates (CS), keratan sulfates (KS), hyaluronan and sialic acids are widely distributed in mammalian tissues [9]. Those anionic glycans serve as facilitators (and sometimes as receptors/co-receptors) to promote pathogen attachment, invasion, assembly, and release to host cells [10, 11]. Many studies have shown that HS, a major component of the mammalian cellular glycocalyx, interacts with SARS-CoV-2 S-protein facilitating entry of virus into host cells [12-14]. Therefore, molecules that interfere with the binding of S-protein to HS have shown effectiveness against SARS-CoV-2. Marine sulfated glycans have drawn much attention as antiviral drug candidates due to their excellent antiviral activity, low cytotoxicity, green renewable sources, and low production costs [15, 16]. We have shown that some marine sulfated glycans exhibit high inhibition activity to previous SARS-CoV-2 strains, such as WT, Delta, and Omicron, by interfering with the binding of viral S-protein to host cell [17-20].

In the current study, the binding of XBB.1.5 S-proteins to heparin (a highly sulfated HS) was analyzed in comparison with the WT version using SPR. A small library, including eight marine sulfated glycans (fucosylated chondroitin sulfates and sulfated fucans derived from marine echinoderm and seaweed, **Figure 1**) and two desulfated derivatives, were prepared to investigate the inhibitory activity of XBB.1.5 S-protein-heparin interactions. We observe that both WT and XBB.1.5 S-proteins bind to heparin with high affinity, and this interaction can be inhibited by several marine-sourced sulfated glycans.

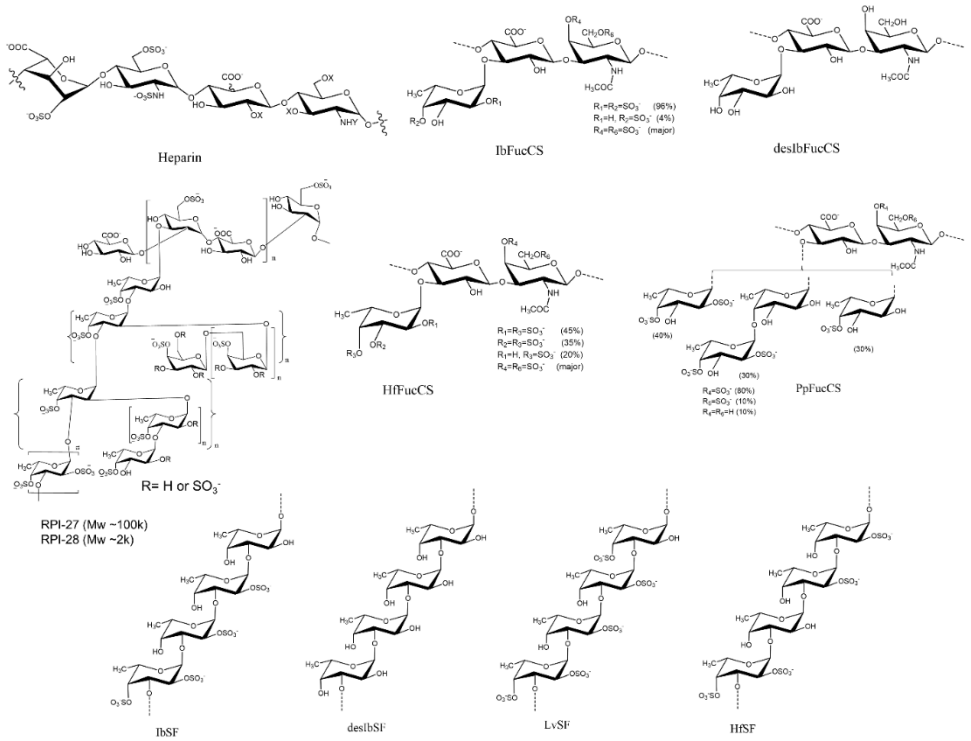

Figure 1. Chemical structures of heparin and marine sulfated glycans.

Preprints (www.preprints.org) | NOT PEER-REVIEWED | Posted: 25 May 2023 doi:10.20944/preprints202305.1749.v1

2. Results

2.1. SARS-CoV-2 Variants and XBB S-protein RBD Mutations

Throughout the Covid-19 pandemic numerous SARS-CoV-2 variants have emerged and posed weighty challenges to both human health and global healthcare systems. Several of these variants are of particular concern due to their increased transmissibility, reduced vaccine and antibody effectiveness and increased virulence. Five variants of concern (VOC) have been declared by the WHO - Alpha (V1, B.1.1.7), Beta (V2, B.1.351), Gamma (V3, P.1), Delta (B.1.617.2) and Omicron (B.1.1.529). The latter was identified in November 2021 both in South Africa and Botswana and named as Omicron [2]. Studies showed that this variant has many mutations leading to an increased risk of reinfection and transmissibility [21, 22]. Omicron rapidly spread worldwide and became the main variant. As the pandemic evolved, a number of new Omicron subvariants emerged, including BA.1, BA.2, BA.2.75, BA.2.12.1, BA.4, BA.5 and XBB (**Figure 2A**). XBB emerged and became predominant in India and Singapore in September 2022, and soon thereafter this variant became the dominant variant in several countries [23]. By the end of 2022, XBB's sublineage XBB.1.5 outcompeted other VOCs, and became the most dominant variant in the USA. Sequence comparison between WT and XBB.1.5 showed that 21 amino acid mutations emerged in the S-protein RBD (Arg319-Phe541, **Figure 2B**). Among these amino acid mutations, XBB.1.5 harbors an F486P substitution, which enables the XBB.1.5 subvariant outcompete other Omicron variants.

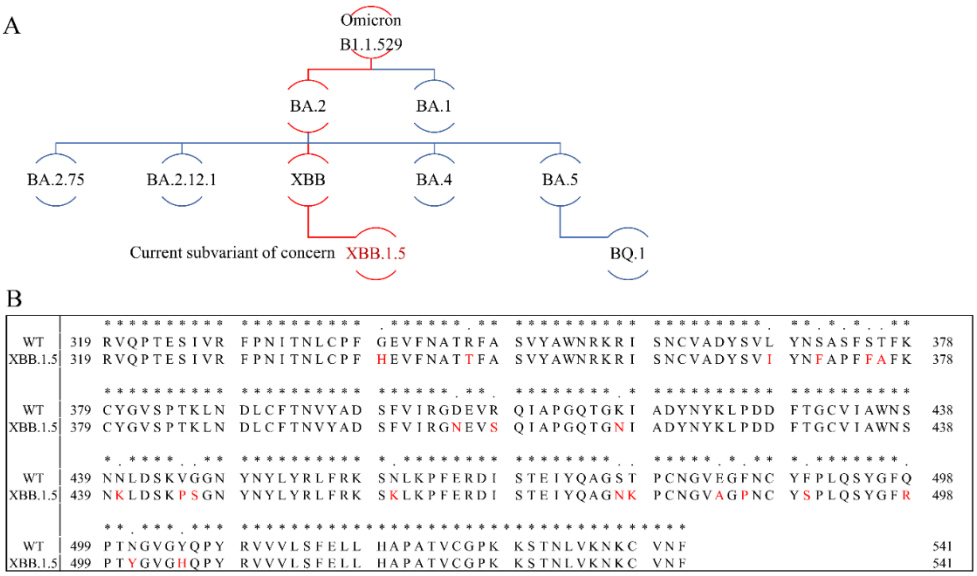

Figure 2. Omicron phylogenetic tree and S-protein RBD amino acid multiple sequence alignment. (A) Omicron phylogenetic tree, adapted from Nextstrain and CoVariants. (B) Mutation profile of S-protein RBD of WT and XBB.1.5 strains. Multiple sequence alignment was carried out by Clustal Omega (1.2.4). Asterisks (*) indicate positions with a single, fully conserved residue.

2.2. Binding Affinity and Kinetics Measurement of Heparin-SARS-CoV-2 S-proteins Interactions

Heparin/HS is a group of highly sulfated, polydisperse anionic linear polysaccharides which consist of variably repeating disaccharide building blocks, D-glucuronic acid (GlcA) or L-iduronic acid linked to N-acetylated or N-sulfated glucosamine [25]. Heparin/HS is widely expressed in the extracellular matrix and on the surface of mammalian cells. Through binding and regulating a wide range of proteins, heparin/HS regulates various biological processes such as blood coagulation, tumor metastasis and pathogen invasion [26]. Heparan sulfates are covalently attached to various core proteins in the extracellular matrix and at the cell surfaces forming HS proteoglycans (HSPGs), which play critical roles in pathogen infection, especially in cellular attachment. Many studies suggest that the highly negatively charged and ubiquitously expressed HSPGs provide an ideal adhesive primary attachment point for viruses [27-29]. Heparin, the highest sulfated GAG, is well

 doi:10.20944/preprints202305.1749.v1

studied as an anticoagulant, and heparin and its analogs are inhibitors to different viruses through blocking viral-HSPGs interactions. Our previous studies showed that full-length heparin and its oligomers can interact with some viral proteins, such as monkeypox A35/A29 proteins, SARS-CoV-2 S-proteins and respiratory syncytial virus glycoproteins [19, 30, 31]. In this study, a heparin SPR chip was prepared to measure the binding kinetics of heparin and S-protein interactions using S-protein RBD from WT and XBB.1.5 variants. Sensorgrams for interactions of heparin with these two S-protein RBDs are shown in **Figure 3**.

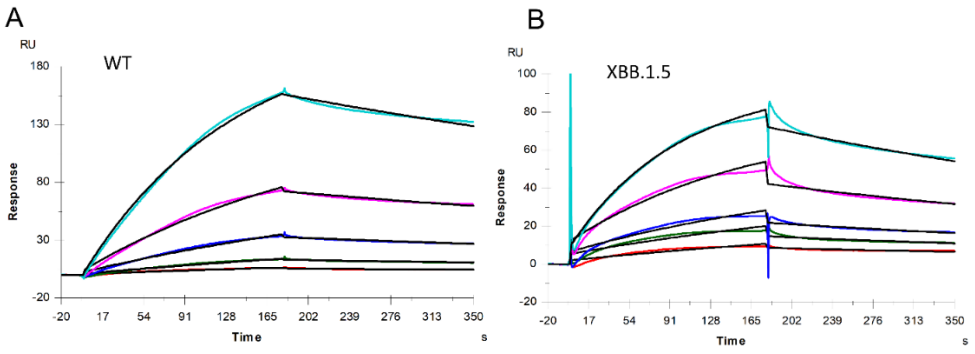

Figure 3. SPR sensorgrams of S-protein RBD of WT and XBB.1.5 binding to heparin. SPR sensorgrams of S-protein RBD binding with heparin; (A) WT and (B) XBB.1.5. Concentrations of S-protein RBD (from top to bottom) are 1000, 500, 250, 125, and 63 nM, respectively.

The binding kinetics and affinity (k_a, association rate constant; k_d, dissociation rate constant; and $K_D=k_a/k_d$, binding equilibrium dissociation constant) between SARS-CoV-2 S-protein RBD (both WT and XBB.1.5) and heparin were obtained by globally fitting the association and dissociation phases using a 1:1 Langmuir binding model. The kinetic parameters of the interaction between SARS-CoV-2 S-protein RBD (WT and XBB.1.5) with heparin are shown in Table 1. The binding affinities of S-protein RBD with heparin are nanomolar: XBB.1.5 (K_D=160 nM) is slightly stronger than WT (K_D=350 nM). From **Figure 2** we can find that among these 20 mutations in the S-protein RBD region, half of the mutations result in reduced amino acid hydrophilicity, while others enhanced the hydrophilicity. Among amino acids from N440 to T500, there are nine mutations, eight of which enhance hydrophilicity. Notably, F486P is known to aid the virus escape the immune system's detection. These relatively concentrated mutations that enhance hydrophilicity could be responsible for XBB.1.5's slightly stronger binding affinities than WT. In addition, interactions between protein and heparin are mainly based on the electrostatic attraction, and therefore, negatively charged GAGs are expected to interact with positively charged amino acids including lysine (K), arginine (R), and histidine (H). Comparing the sequences of S-protein of XBB with WT (**Figure 2**), an additional six positively charged amino acid residues are found on the XBB RBD, which can enhance heparin binding affinity.

Table 1. Kinetic data of interactions of S-protein RBD of WT and XBB.1.5 with heparin*.

	k_a ($M^{-1}s^1$)	k_d (1/s)	K_D (M)
WT	3.3×10^3 (±21)	1.2×10^{-3} ($\pm 4.1 \times 10^{-6}$)	3.5×10^{-7}
XBB	2.1×10^4 (±250)	3.4×10^{-3} ($\pm 2.3 \times 10^{-5}$)	1.6×10^{-7}

* The data with (±) in parentheses are the standard deviations (SD) from global fitting of five injections.

2.3. SPR Solution Competition between Surface-Immobilized Heparin and Isostichopusbadionotus-sourced Sulfated Glycans IbSF, IbSFucCS, desIbSF and desIbFucCS

Two sulfated glycans, sulfated fucan (IbSF) and fucosylated chondroitin sulfate (IbSFucCS), were originally isolated and characterized from *Isostichopus badionotus* (a species of sea cucumber in

 doi:10.20944/preprints202305.1749.v1

the family Stichopodidae) by Chen et.al [32, 33]. The structure of IbSF is [→3)-α-Fuc2,4S-(1→3)-α-Fuc2S-(1→3)-α-Fuc2S-(1→3)-α-Fuc-(1→]$_n$ and IbFucCS's structure is of [→3)-β-GalNAc4,6S-(1→4)β-GlcA[(3→1)Y]-(1→]$_n$, where Y = α-Fuc2,4S (96%) or α-Fuc4S (4%) (**Figure 1**). Both IbSF and IbFucCS showed good anticoagulant and antithrombotic activities. Our previous study demonstrated that these two marine sulfated glycans also were promising inhibitors towards monkeypox virus (MPXV). Their fully chemical desulfated derivatives, desulfated IbSF (desIbSF) and IbFucCS (desIbFucCS) were prepared as described previously [34], and showed weak competitive inhibition activity between heparin and MPXV A29 and A35 proteins [19]. Pomin's group indicated that IbSF and IbFucCS showed excellent anti-SARS-CoV-2 activity on both WT and Delta variants, by disrupting the entry of virus into the host cells [17].

SPR was used to perform solution/surface competition experiments for studying the ability of Isostichopus badionotus-sourced glycans (IbSF, IbFucCS, desIbSF and IbFucCS) to inhibit the interactions between SARS-CoV-2 S-proteins (WT and XBB.1.5) and immobilized heparin (**Figure 4A,C**). The same concentration of Ib glycans (5 μg/mL) was mixed with 1 μM S-proteins (WT and XBB.1.5 individually). Both Ib-sourced sulfated glycans, IbSF and IbFucCS, significantly inhibited the binding of surface-immobilized heparin to the S-proteins (WT and XBB.1.5). Soluble heparin inhibited the binding of WT and XBB.1.5 SARS-CoV-2 S-protein to surface-immobilized heparin by 53.4% and 54.6%, respectively (**Figure 4B**,**D**). IbSF and IbFucCS had a better result on the inhibition of immobilized heparin binding to WT S-protein, with 94.8% and 99.5%, respectively. At the same time, IbSF and IbFucCS also showed very strong inhibition activity, with normalized XBB. 1.5 ratio of 92.5% and 91.3%, respectively. The fully chemical desulfated derivatives, desIbSF and desIbFucCS, showed significantly lower competitive inhibition of heparin binding to both WT and XBB.1.5 S-proteins. Our results indicate that sulfation of these marine-sourced glycans play a critical role in the interaction of S-proteins and their anti-SARS-CoV-2 activity.

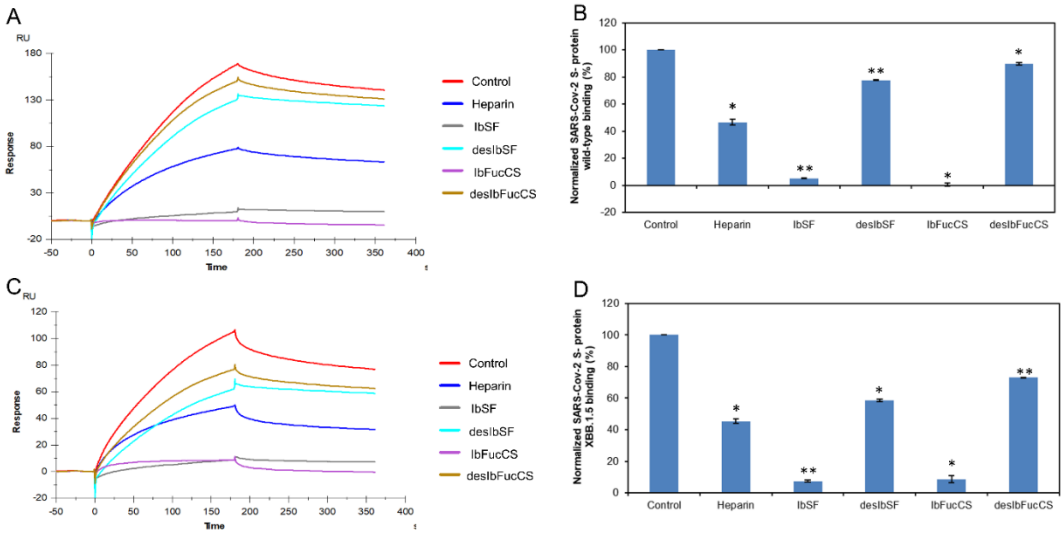

Figure 4. Solution competition between heparin and Ib glycans. (A) SPR sensorgrams of the WT SARS-CoV-2 S-protein–heparin interaction competing with different Ib glycans. The concentration of the WT SARS-CoV-2 S-protein was 1 μM mixed with 5 μg/mL of different Ib glycans. (B) Bar graphs (based on triplicate experiments with standard deviation) of normalized WT SARS-CoV-2 S-protein binding preference to surface heparin by competing with different Ib glycans. (C) SPR sensorgrams of the XBB.1.5 SARS-CoV-2 S-protein–heparin interaction competing with different Ib glycans. The concentration of the the XBB.1.5 SARS-CoV-2 S-protein was 1 μM mixed with 5 μg/mL of different Ib glycans. (D) Bar graphs (based on triplicate experiments with standard deviations) of the normalized XBB.1.5 SARS-CoV-2 S-protein binding preference to surface heparin by competing with different Ib glycans. Statistical analysis was performed using an unpaired two-tailed t-test (*: $p \leq 0.05$ compared with the control, **: $p \leq 0.01$ compared with the control).

 doi:10.20944/preprints202305.1749.v1

2.4. SPR Solution Competition between Surface-Immobilized Heparin and Holothuria floridana-Sourced Glycans HfSF and HfFucCS

Two marine-sulfated glycans, HfSF and HfFucCS, from the sea cucumber Holothuriafloridana (Hf) were firstly reported by Shi et al. 2019. HfSF is a sulfated fucan whose structure is [→3)-α-Fuc2,4S-(1→3)-α-Fuc-(1→3)-α-Fuc2S-(1→3)-α-Fuc2S-(1→]$_n$, while HfFucCS is a fucosylated chondroitin sulfate structure with the following structure [→3)-β-GalNAc4,6S-(1→4)-β-GlcA-[(3→1)Y]-(1→]$_n$, where Y = αFuc2,4S (45%), α-Fuc3,4S (35%), or α-Fuc4S (20%) [35] (**Figure 1**). These two Hf glycans were reported to have good inhibition activities towards some SARS-CoV-2 variants and MPXV [17, 19].

Again, we used solution/surface competition SPR experiments for studying the ability of HfSF and HfFucCS to inhibit the interactions between SARS-CoV-2 S-proteins (WT and XBB.1.5) and immobilized heparin. The same concentration of Hf glycans (5 μg/mL) was mixed with 1 μM S-proteins (WT and XBB.1.5 individually). Solution competition SPR results are shown in **Figure 5A,C.** Heparin inhibited the binding of WT and XBB.1.5 S-proteins binding to surface-immobilized heparin by 53.4% and 54.5%, respectively. HfSF and HfFucCS showed excellent activity for the inhibition of WT S-protein binding to surface-immobilized heparin, with 88.9% and 93.1%, respectively. Meanwhile, HfSF and HfFucCS also showed good results for the inhibitions of XBB.1.5 S-protein binding to surface-immobilized heparin, with 84.0% and 83.8%, respectively (**Figure 5B,D**).

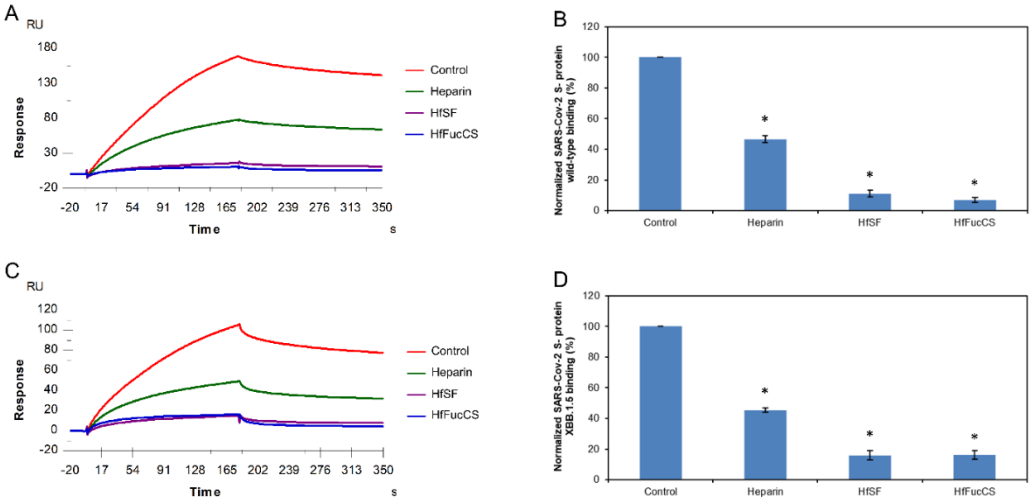

Figure 5. Solution competition between heparin and Hf glycans. (A) SPR sensorgrams of the WT SARS-CoV-2 S-protein–heparin interaction competing with different Hf glycans. The concentration of the WT SARS-CoV-2 S-protein was 1 μM mixed with 5 μg/mL of different Hf glycans. (B) Bar graphs (based on triplicate experiments with standard deviation) of normalized WT SARS-CoV-2 S-protein binding preference to surface heparin by competing with different Hf glycans. (C) SPR sensorgrams of the XBB.1.5 SARS-CoV-2 S-protein–heparin interaction competing with different Hf glycans. The concentration of the XBB.1.5 SARS-CoV-2 S-protein was 1 μM mixed with 5 μg/mL of different Hf glycans. (D) Bar graphs (based on triplicate experiments with standard deviations) of the normalized XBB.1.5 SARS-CoV-2 S-protein binding preference to surface heparin by competing with different Hf glycans. Statistical analysis was performed using an unpaired two-tailed t-test (*: $p \leq 0.05$ compared with the control).

2.5. SPR Solution Competition between Surface-Immobilized Heparin and two Marine-Soured Sulfated Glycans LvSF and PpFucCS

Sulfated fucan LvSF is a polysaccharide isolated from the sea urchin *Lytechinus variegatus* with the structure of [→3)-α-Fuc2,4S-(1→3)-αFuc2S-(1→3)-α-Fuc2S-(1→3)-α-Fuc4S-(1→]$_n$ [36], while the fucosylated chondroitin sulfate PpFucCS is isolated from the sea cucumber *Pentacta pygmaea* with a structure of [→3)-β-GalNAcX(1→4)-β-GlcA-[(3→1)Y]-(1→]$_n$, where X = 4S (80%), 6S (10%), or non-

 doi:10.20944/preprints202305.1749.v1

sulfated (10%), and Y = α-Fuc2,4S (40%), αFuc2,4S(1→4)-α-Fuc (30%), or α-Fuc4S (30%) (**Figure 1**) [37].

SPR was applied to perform solution/ surface competition experiments for studying the ability of the marine-sourced glycans LvSF and PpFucCS to inhibit the interactions between SARS-CoV-2 S-proteins (WT and XBB.1.5) and immobilized heparin. The same concentration of Hf glycans (5 μg/mL) was mixed with 1 μM S-proteins (WT and XBB.1.5 individually). Solution competition results between these marine-sourced glycans and heparin are indicated in **Figure 6A,C**. Heparin inhibited the binding of WT and XBB.1.5 S-proteins binding to surface-immobilized heparin by 53.4% and 54.5%, respectively. PpFucCS and LvSF showed excellent results for the inhibitions of WT S-protein binding to surface-immobilized heparin, with 97.9% and 86.0%, respectively. Meanwhile, PpFucCS and LvSF also showed good results for the inhibitions of XBB.1.5 S-protein binding to surface-immobilized heparin, with 91/5% and 88.6%, respectively (**Figure 6B,D**).

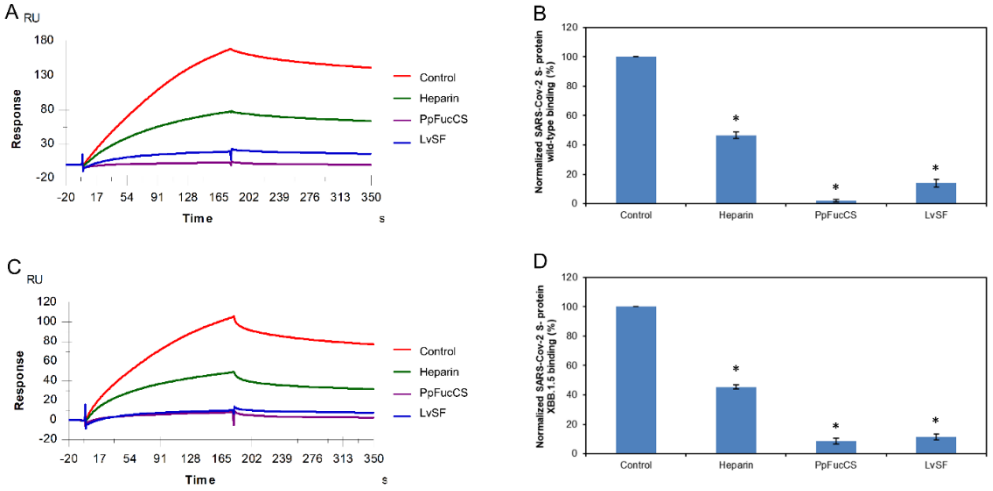

Figure 6. Solution competition between heparin and PpFucCS and LvSF. (A) SPR sensorgrams of the WT SARS-CoV-2 S-protein–heparin interaction competing with different PpFucCS and LvSF. The concentration of the WT SARS-CoV-2 S-protein was 1 μM mixed with 5 μg/mL of different PpFucCS and LvSF glycans. (B) Bar graphs (based on triplicate experiments with standard deviation) of normalized WT SARS-CoV-2 S-protein binding preference to surface heparin by competing with different PpFucCS and LvSF glycans. (C) SPR sensorgrams of the XBB.1.5 SARS-CoV-2 S-protein–heparin interaction competing with different PpFucCS and LvSF glycans. The concentration of the the XBB.1.5 SARS-CoV-2 S-protein was 1 μM mixed with 5 μg/mL of different PpFucCS and LvSF glycans. (D) Bar graphs (based on triplicate experiments with standard deviations) of the normalized XBB.1.5 SARS-CoV-2 S-protein binding preference to surface heparin by competing with different PpFucCS and LvSF glycans. Statistical analysis was performed using an unpaired two-tailed t-test (*: $p \leq 0.05$ compared with the control).

2.6. SPR Solution Competition between Surface-Immobilized Heparin and two Marine-Soured Sulfated Glycans RPI-27 and RPI-28

RPI-27 and RPI-28 are a family of sulfated heteropolysaccharides derived from the brown seaweed *Saccharina japonica* consisting of two types of polysaccharide backbones: (1) a sulfated glucuronomannan and a glucuronomannan backbone with repeating 4-linked GlcA and 2-linked mannose (Man), and a Man residue with the first C-6 sulfated mannopyranose residue from the nonreducing terminus (2) a glucuronan with a backbone of 3-linked GlcA. There are some other branched chains including GlcA-(1→3)-Man-(1→4)-GlcA, Man-(1→3)-GlcA-(1→4)-GlcA, Fuc-(1→4)-GlcA and Fuc-(1→3)-Fuc. (Figure 1) [38]. RPI-27 and RPI-28 share the same structure but have a different average molecular weight with 100 kDa and 12 kDa respectively.

In this competition SPR analysis, the same concentration of RPI-27 and RPI-28 glycans (50nM) was mixed with 1 μM S-proteins (WT and XBB.1.5 individually). Solution competition results between these glycans and heparin are shown in **Figure 7A,C**. Heparin inhibited the binding of WT

 doi:10.20944/preprints202305.1749.v1

and XBB.1.5 S-proteins binding to surface-immobilized heparin by 53.4% and 54.6%, respectively. RPI-27 and RPI-28 showed better results for inhibition of WT S-protein binding to surface-immobilized heparin, with 83.7% and 75.4%, respectively. Meanwhile, RPI-27 and RPI-28 also showed good results for the inhibitions of XBB.1.5 S-protein binding to surface-immobilized heparin, with 68.3% and 74.4%, respectively (**Figure 7B,D**).

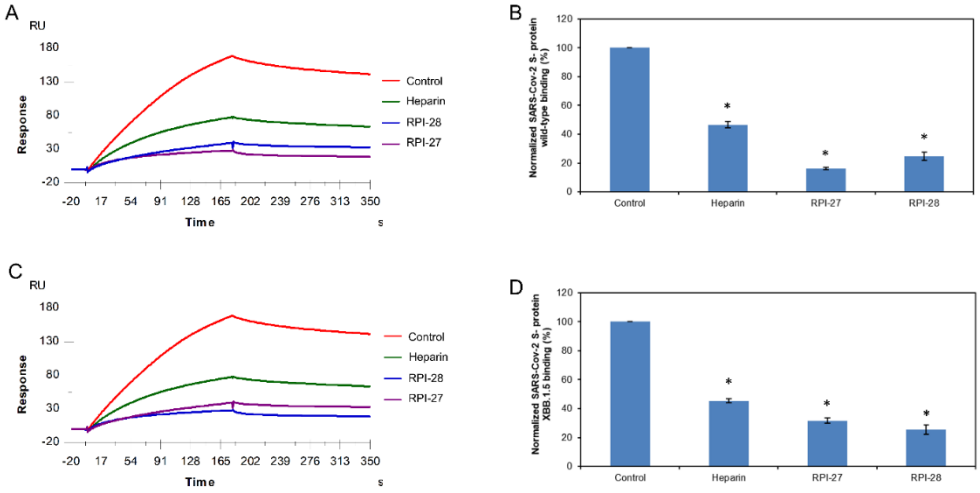

Figure 7. Solution competition between heparin and RPI-27/ RPI-28. (A) SPR sensorgrams of the WT SARS-CoV-2 S-protein–heparin interaction competing with RPI-27/ RPI-28. The concentration of the WT SARS-CoV-2 S-protein was 1μM mixed with 5 μg/mL of different RPI-27/ RPI-28 glycans. (B) Bar graphs (based on triplicate experiments with standard deviation) of normalized WT SARS-CoV-2 S-protein binding preference to surface heparin by competing with different RPI-27/ RPI-28 glycans. (C) SPR sensorgrams of the XBB.1.5 SARS-CoV-2 S-protein–heparin interaction competing with different RPI-27/ RPI-28 glycans. The concentration of the the XBB.1.5 SARS-CoV-2 S-protein was 1μM mixed with 5 μg/mL of different RPI-27/ RPI-28 glycans. (D) Bar graphs (based on triplicate experiments with standard deviations) of the normalized XBB.1.5 SARS-CoV-2 S-protein binding preference to surface heparin by competing with different RPI-27/ RPI-28 glycans. Statistical analysis was performed using an unpaired two-tailed t-test (*: $p \leq 0.05$ compared with the control).

All eight naturally occurring marine-sourced sulfated glycans (IbSF, IbFucCS, HfSF, HfFucCS, PpFucCS, LvSF, RPI-27, PRI-28) showed the ability to inhibit the interactions between SARS-CoV-2 S-proteins (both WT and XBB.1.5) and surface-immobilized heparin. However, the chemically desulfated glycans, both desIbSF and desIbFucCS, showed significantly reduced binding activity of both S-proteins to surface-immobilized heparin (**Table 2**). Our study shows that sulfation plays critical roles in the inhibitory activity of marine sulfated glycans. All eight naturally occurring marine-sourced sulfated glycans exhibited outstanding inhibition activity against surface-immobilized heparin binding with WT and XBB. 1.5 SARS-CoV-2 S-proteins. Among the three different marine-sourced fucosylated chondroitin sulfates, IbFucCS had the highest sulfation level (96% branching disulfated fucoses) and exhibited the best inhibitory activity towards WT S-protein. HfFucCS (80% branching disulfated fucoses) shows slightly better inhibitory activity than PpFucCS (70% branching disulfated fucoses) against both WT and XBB.1.5. Clearly, sulfation levels are an important factor for the inhibitory activities of marine-sourced FucCS glycans. Despite sharing the same fucan tetrasaccharide repeating unit, IbSF, LvSF and HfSF differ in their sulfation patterns. The higher sulfated LvSF has pentasulfated tetrasaccharide building blocks, while IbSF and HfSF have tetrasulfated tetrasaccharide building blocks. Among them, IbSF showed the best inhibitory activity, while LvSF and HfSF showed very similar inhibitory activities. This suggests that sulfation pattern has a more pronounced influence on the interactions with SARS-CoV-2 S-proteins than the degree of sulfation. RPI-27 and RPI-28 showed similar inhibitory activity, indicating that no obvious correlations between this seaweed-derived fucoidan molecular weight and binding properties. Despite the strong inhibitory activity of all tested sulfated glycans against both viral proteins in the

 doi:10.20944/preprints202305.1749.v1

SPR-based binding to the surface-immobilized heparin, there are no clear correlations between the structural features of these glycans and their binding properties. Similar results were found in our previous study on the inhibitory activity of these sulfated glycans against other evolving SARS-CoV-2 strains and Monkeypox virus [17, 19].

Table 2. Summary of solution competition between heparin and eight marine-derived glycans binding to S-proteins [a].

Normalized S-protein binding	Control[b]	Heparin	IbSF	desIbSF	IbFucCS	desIbFucCS
WT (%)	100	46.6*	5.2**	77.7**	0.5*	89.8*
XBB.1.5 (%)	100	45.4*	7.5**	58.4*	8.7*	72.9**
Normalized S-protein binding	**HfSF**	**HfFucCS**	**PpFucCS**	**LvSF**	**RPI-27**	**RPI-28**
WT (%)	11.1*	6.9*	2.1*	14.0*	16.3*	24.6*
XBB.1.5 (%)	16.0*	16.2*	8.5*	11.4*	31.7*	25.5*

[a]SPR sensorgrams of WT/XXB.1.5 S-protein–heparin interaction competing with 10 different marine-derived glycans. The concentration of proteins was 1 μM mixed with 5 μg/mL of different glycans. [b]The control had the same concentration of WT/XXB.1.5 S-protein (1 μM) without any mixed glycans. Statistical analysis was performed using an unpaired two-tailed t-test (*: $p \leq 0.05$ compared with the control, **: $p \leq 0.01$ compared with the control).

3. Materials and Methods

3.1. Materials

Eight marine-sourced sulfated glycans (IbSF, desIbSF, IbFucCS, desIbFucCS, PpFucCS, LvSF, HfSF, HfFucCS) from the sea cucumbers *I. badionotus* and *P. pygmaea, sea urchin L. variegatus*, and the Florida sea cucumber *Holothuria floridana* were provided from Dr. Pomin's lab at the University of Mississippi. Two seaweeds originated sulfated glycans (RPI-27 and RPI-28) were purified in Dr. Jin's Lab from seaweed *Saccharina japonica*. SARS-CoV-2 S-protein RBD WT expressed in Expi293F cells was provided by the Bates lab, University of Mississippi. SARS-CoV-2 S-protein RBD XBB.1.5 was purchased from Sino Biological Inc. (Wayne, PA, USA). The recombinant WT S-protein consists of 234 amino acids and has a predicted molecular mass of 26.72 kDa. The recombinant XBB.1.5 S-protein consists of 234 amino acids and has a predicted molecular mass of 26.58 kDa (see the amino acid sequences in Figure 2). Porcine intestinal heparin (average molecular weight of 15 kDa) was purchased from Celsus Laboratories (Cincinnati, OH, USA). Streptavidin (SA) sensor chips were purchased from Cytiva (Uppsala, Sweden). SPR measurements were performed on a BIAcore T200 or 3000 SPR (Uppsala, Sweden), and Biaevaluation software (version 4.0.1 or 3.2) was used for data processing.

3.2. Preparation of Heparin SPR chips

The biotinylated heparin was obtained by employing the following method: 2 mg heparin and 2 mg amine-PEG_3-Biotin (Thermo Scientific, Waltham, MA, USA) were mixed in 200 μL water, following 10 mg NaCNBH3 was added into the mixture. The solution was incubated at 70 °C for 24 h, after that another 10 mg $NaCNBH_3$ was added, and the mixture was incubated at 70 °C for another 24 h. Once the reaction was finished, the mixture underwent desalting using a spin column (3000 molecular weight cut-off). Biotinylated heparin was lyophilized for the preparation of biochip. A heparin chip for the SPR study was made using the following protocol: a 20 μL solution of biotinylated heparin (0.1 mg/mL) in HBS-EP^+ buffer was carefully introduced into flow cells 2 to 4 of the SA chip at a flow rate of 10 μL/min. In addition, the immobilization of flow cell 1 was carried out by employing biotin as a reference channel, following the same procedure.

3.3. Binding Kinetics and Affinity Studies of the Interaction between Heparin and the SARS-CoV-2 S-protein

The S-protein RBD was diluted in HBS-EP+ buffer (10 mM HEPES, 150 mM NaCl and 0.05% v/v Surfactant P20, pH 7.4). Different dilutions of S-protein RBD were injected at a flow rate of 30 μL/min. At the end of each injection, the same buffer flowed over the sensor surface for 3 min to facilitate dissociation. The SPR chip was regenerated by injecting 30 μL of 2 M NaCl to flow each channel. All responses were monitored as sensorgrams at 25 °C.

3.4. Inhibition Activity of the Marine Sulfated Glycans on Heparin–SARS-CoV-2 S-protein Interactions

To evaluate the inhibition of the SARS-CoV-2 S-protein–heparin interaction, 1 μM of S-protein RBD was premixed with 5 μg/mL of different glycans in HBS-EP+ buffer (pH 7.4) and injected over the heparin chip at a flow rate of 30 μL/min. The sensor surface was regenerated using a 30 μL injection of a 2 M NaCl solution. S-protein RBD was used in the control experiment to verify the complete regeneration of the sensor surface.

4. Conclusions

SARS-CoV-2 S-proteins (WT and XBB.1.5) strongly bound to surface immobilized heparin. SPR competition assays were conducted to analyze the solution competition between surface-immobilized heparin and ten marine sulfated glycans (IbSF, desIbSF, IbFucCS, desIbFucCS, PpFucCS, LvSF, HfSF, HfFucCS, RPI-27 and RPI-28) derived from sea cucumber and seaweed. Our finding demonstrated that all the eight naturally occurring marine-sourced sulfated glycans (IbSF, IbFucCS, , PpFucCS, LvSF, HfSF, HfFucCS, RPI-27 and RPI-28) provided striking inhibitory activity of chip-surface heparin binding to the WT and WT S-proteins. However, the inhibitory activity of fully desulfated IbSF (desIbSF) and fully desulfated IbFucCS (desIbFucCS) was found to be very low. This data reveals that the sulfated glycans derived from sea cucumbers and seaweed exhibit great potential as natural inhibitors of evolving variants of SARS-CoV-2 by efficiently binding to viral S-proteins. The study of molecular interactions, particularly the degree of sulfation, will pave the way for developing new therapeutics for the prevention and treatment of the rapidly evolving SARS-CoV-2.

Author Contributions: Conceptualization, F.Z. and R.J.L.; methodology, P.H, D.S.; analysis, P.H, Y.L.; resource, S.K., R.D., V.H.P., M.F.; W.J.; J.B; original draft preparation, P.H, Y.L., F.Z; review and editing, K.X., V.H.P., J.B.; J.S.D. and R.J.L.; revision, P.H., V.H.P., F.Z. and R.J.L., funding acquisition, J.S.D., V.H.P., F.Z. and R.J.L. All authors have read and agreed to the published version of the manuscript.

Funding: This work was supported by NIH (S10OD028523, R21AI156573 (R.J.L, F.Z.), 1P20GM130460-01A1-7936 and 1R03NS110996-01A1 (V.H.P.); (GlycoMIP a National Science Foundation Materials Innovation Platform funded through Cooperative Agreement DMR-1933525 (R.J.L., J.S.D., F.Z.), and New York State Biodefense Commercialization Fund (J.S.D., F.Z).

Data Availability Statement: Data presented in this study are available on request.

Conflicts of Interest: The authors declare no conflict of interest.

References

1. WHO Coronavirus (COVID-19) Dashboard. Available online: https://covid19.who.int/ (accessed on 20 April 2023).
2. Tracking SARS-CoV-2 Variants. Available online https://www.who.int/activities/tracking-SARS-CoV-2-variants (accessed on 20 April 2023).
3. Provisional Mortality Data — United States, 2022. Available online.
4. Bakhshandeh, B.; Jahanafrooz, Z.; Abbasi, A.; Goli, M. B.; Sadeghi, M.; Mottaqi, M. S.; Zamani, M., Mutations in SARS-CoV-2; Consequences in structure, function, and pathogenicity of the virus. Microbial Pathogenesis 2021, 154, 104831.
5. Zhou, Y.; Zhi, H.; Teng, Y., The outbreak of SARS-CoV-2 Omicron lineages, immune escape, and vaccine effectivity. J Med Virol 2023, 95, (1), e28138.
6. COVID Data Tracker. Available online https://covid.cdc.gov/covid-data-tracker/#variant-proportions. (accessed on 20 April 2023).

7. Qu, P.; Faraone, J. N.; Evans, J. P.; Zheng, Y.-M.; Carlin, C.; Anghelina, M.; Stevens, P.; Fernandez, S.; Jones, D.; Panchal, A. R.; Saif, L. J.; Oltz, E. M.; Zhang, B.; Zhou, T.; Xu, K.; Gumina, R. J.; Liu, S.-L., Enhanced evasion of neutralizing antibody response by Omicron XBB.1.5, CH.1.1, and CA.3.1 variants. Cell Reports 2023, 42, (5), 112443
8. Uriu, K.; Ito, J.; Zahradnik, J.; Fujita, S.; Kosugi, Y.; Schreiber, G.; Genotype to Phenotype Japan, C.; Sato, K., Enhanced transmissibility, infectivity, and immune resistance of the SARS-CoV-2 omicron XBB.1.5 variant. Lancet Infect Dis 2023, 23, (3), 280-281.
9. Gandhi, N. S.; Mancera, R. L., The Structure of Glycosaminoglycans and their Interactions with Proteins. Chemical Biology & Drug Design 2008, 72, (6), 455-482.
10. Kamhi, E.; Joo, E. J.; Dordick, J. S.; Linhardt, R. J., Glycosaminoglycans in infectious disease. Biological Reviews 2013, 88, (4), 928-943.
11. Aquino, R. S.; Park, P. W., Glycosaminoglycans and infection. FBL 2016, 21, (6), 1260-1277.
12. Kearns, F. L.; Sandoval, D. R.; Casalino, L.; Clausen, T. M.; Rosenfeld, M. A.; Spliid, C. B.; Amaro, R. E.; Esko, J. D., Spike-heparan sulfate interactions in SARS-CoV-2 infection. Current Opinion in Structural Biology 2022, 76, 102439.
13. Chittum, J. E.; Sankaranarayanan, N. V.; O'Hara, C. P.; Desai, U. R., On the Selectivity of Heparan Sulfate Recognition by SARS-CoV-2 Spike Glycoprotein. ACS Medicinal Chemistry Letters 2021, 12, (11), 1710-1717.
14. Yan, L.; Song, Y.; Xia, K.; He, P.; Zhang, F.; Chen, S.; Pouliot, R.; Weiss, D. J.; Tandon, R.; Bates, J. T.; Ederer, D. R.; Mitra, D.; Sharma, P.; Davis, A.; Linhardt, R. J., Heparan sulfates from bat and human lung and their binding to the spike protein of SARS-CoV-2 virus. Carbohydrate Polymers 2021, 260, 117797.
15. Kang, H.-K.; Seo, C. H.; Park, Y., The Effects of Marine Carbohydrates and Glycosylated Compounds on Human Health. International Journal of Molecular Sciences 2015, 16, (3), 6018-6056.
16. Arokiarajan, M. S.; Thirunavukkarasu, R.; Joseph, J.; Ekaterina, O.; Aruni, W., Advance research in biomedical applications on marine sulfated polysaccharide. International Journal of Biological Macromolecules 2022, 194, 870-881.
17. Dwivedi, R.; Sharma, P.; Farrag, M.; Kim, S. B.; Fassero, L. A.; Tandon, R.; Pomin, V. H., Inhibition of SARS-CoV-2 wild-type (Wuhan-Hu-1) and Delta (B.1.617.2) strains by marine sulfated glycans. Glycobiology 2022, 32, (10), 849-854.
18. Song, Y.; He, P.; Rodrigues, A. L.; Datta, P.; Tandon, R.; Bates, J. T.; Bierdeman, M. A.; Chen, C.; Dordick, J.; Zhang, F.; Linhardt, R. J., Anti-SARS-CoV-2 Activity of Rhamnan Sulfate from Monostroma nitidum. Marine Drugs 2021, 19, (12), 685.
19. He, P.; Shi, D.; Li, Y.; Xia, K.; Kim, S. B.; Dwivedi, R.; Farrag, M.; Pomin, V. H.; Linhardt, R. J.; Dordick, J. S.; Zhang, F., SPR Sensor-Based Analysis of the Inhibition of Marine Sulfated Glycans on Interactions between Monkeypox Virus Proteins and Glycosaminoglycans. Marine Drugs 2023, 21, (5), 264.
20. Kwon, P. S.; Oh, H.; Kwon, S.-J.; Jin, W.; Zhang, F.; Fraser, K.; Hong, J. J.; Linhardt, R. J.; Dordick, J. S., Sulfated polysaccharides effectively inhibit SARS-CoV-2 in vitro. Cell Discovery 2020, 6, (1), 50.
21. Guo, D.; Duan, H.; Cheng, Y.; Wang, Y.; Hu, J.; Shi, H., Omicron-included mutation-induced changes in epitopes of SARS-CoV-2 spike protein and effectiveness assessments of current antibodies. Molecular Biomedicine 2022, 3, (1), 12.
22. Wang, Q.; Iketani, S.; Li, Z.; Liu, L.; Guo, Y.; Huang, Y.; Bowen, A. D.; Liu, M.; Wang, M.; Yu, J.; Valdez, R.; Lauring, A. S.; Sheng, Z.; Wang, H. H.; Gordon, A.; Liu, L.; Ho, D. D., Alarming antibody evasion properties of rising SARS-CoV-2 BQ and XBB subvariants. Cell 2023, 186, (2), 279-286.e8.
23. Tamura, T.; Ito, J.; Uriu, K.; Zahradnik, J.; Kida, I.; Nasser, H.; Shofa, M.; Oda, Y.; Lytras, S.; Nao, N.; Itakura, Y.; Deguchi, S.; Suzuki, R.; Wang, L.; Begum, M. M.; Tsuda, M.; Kosugi, Y.; Fujita, S.; Yoshimatsu, K.; Suzuki, S.; Asakura, H.; Nagashima, M.; Sadamasu, K.; Yoshimura, K.; Yamamoto, Y.; Nagamoto, T.; Schreiber, G.; Consortium, T. G. t. P. J.; Ikeda, T.; Fukuhara, T.; Saito, A.; Tanaka, S.; Matsuno, K.; Takayama, K.; Sato, K., Virological characteristics of the SARS-CoV-2 XBB variant derived from recombination of two Omicron subvariants. bioRxiv 2022, 2022.12.27.521986.
24. Yue, C.; Song, W.; Wang, L.; Jian, F.; Chen, X.; Gao, F.; Shen, Z.; Wang, Y.; Wang, X.; Cao, Y., ACE2 binding and antibody evasion in enhanced transmissibility of XBB.1.5. The Lancet Infectious Diseases 2023, 23, (3), 278-280.
25. Muñoz, E. M.; Linhardt, R. J., Heparin-Binding Domains in Vascular Biology. Arteriosclerosis, Thrombosis, and Vascular Biology 2004, 24, (9), 1549-1557.
26. Weiss, R. J.; Esko, J. D.; Tor, Y., Targeting heparin and heparan sulfate protein interactions. Organic & Biomolecular Chemistry 2017, 15, (27), 5656-5668.
27. De Pasquale, V.; Quiccione, M. S.; Tafuri, S.; Avallone, L.; Pavone, L. M., Heparan Sulfate Proteoglycans in Viral Infection and Treatment: A Special Focus on SARS-CoV-2. International Journal of Molecular Sciences 2021, 22, (12), 6574.

28. Shafti-Keramat, S.; Handisurya, A.; Kriehuber, E.; Meneguzzi, G.; Slupetzky, K.; Kirnbauer, R., Different Heparan Sulfate Proteoglycans Serve asCellular Receptors for HumanPapillomaviruses. Journal of Virology 2003, 77, (24), 13125-13135.
29. Liu, J.; Thorp, S. C., Cell surface heparan sulfate and its roles in assisting viral infections. Medicinal Research Reviews 2002, 22, (1), 1-25.
30. Shi, D.; Bu, C.; He, P.; Song, Y.; Dordick, J. S.; Linhardt, R. J.; Chi, L.; Zhang, F., Structural Characteristics of Heparin Binding to SARS-CoV-2 Spike Protein RBD of Omicron Sub-Lineages BA.2.12.1, BA.4 and BA.5. Viruses 2022, 14, (12).
31. Shi, D.; He, P.; Song, Y.; Linhardt, R. J.; Dordick, J. S.; Chi, L.; Zhang, F., Interactions of heparin with key glycoproteins of human respiratory syncytial virus. Frontiers in Molecular Biosciences 2023, 10.
32. Chen, S.; Hu, Y.; Ye, X.; Li, G.; Yu, G.; Xue, C.; Chai, W., Sequence determination and anticoagulant and antithrombotic activities of a novel sulfated fucan isolated from the sea cucumber Isostichopus badionotus. Biochimica et Biophysica Acta (BBA) - General Subjects 2012, 1820, (7), 989-1000.
33. Chen, S.; Xue, C.; Yin, L. a.; Tang, Q.; Yu, G.; Chai, W., Comparison of structures and anticoagulant activities of fucosylated chondroitin sulfates from different sea cucumbers. Carbohydrate Polymers 2011, 83, (2), 688-696.
34. Castro, M. O.; Pomin, V. H.; Santos, L. L.; Vilela-Silva, A.-C. E. S.; Hirohashi, N.; Pol-Fachin, L.; Verli, H.; Mourão, P. A. S., A Unique 2-Sulfated β-Galactan from the Egg Jelly of the Sea Urchin Glyptocidaris crenularis. Journal of Biological Chemistry 2009, 284, (28), 18790-18800.
35. Shi, D.; Qi, J.; Zhang, H.; Yang, H.; Yang, Y.; Zhao, X., Comparison of hydrothermal depolymerization and oligosaccharide profile of fucoidan and fucosylated chondroitin sulfate from Holothuria floridana. International Journal of Biological Macromolecules 2019, 132, 738-747.
36. Mulloy, B.; Ribeiro, A. C.; Alves, A. P.; Vieira, R. P.; Mourão, P. A., Sulfated fucans from echinoderms have a regular tetrasaccharide repeating unit defined by specific patterns of sulfation at the 0-2 and 0-4 positions. Journal of Biological Chemistry 1994, 269, (35), 22113-22123.
37. Dwivedi, R.; Samanta, P.; Sharma, P.; Zhang, F.; Mishra, S. K.; Kucheryavy, P.; Kim, S. B.; Aderibigbe, A. O.; Linhardt, R. J.; Tandon, R.; Doerksen, R. J.; Pomin, V. H., Structural and kinetic analyses of holothurian sulfated glycans suggest potential treatment for SARS-CoV-2 infection. Journal of Biological Chemistry 2021, 297, (4), 101207 .
38. Jin, W.; Wang, J.; Ren, S.; Song, N.; Zhang, Q., Structural Analysis of a Heteropolysaccharide from Saccharina japonica by Electrospray Mass Spectrometry in Tandem with Collision-Induced Dissociation Tandem Mass Spectrometry (ESI-CID-MS/MS). Marine Drugs 2012, 10, (10), 2138-2152.